Ongoing introgression of a secondary sexual plumage trait in a stable avian hybrid zone

Kira M. Long[1*], Angel G. Rivera-Colón[2], Kevin F. P. Bennett[3,4], Julian M. Catchen[2], Michael J. Braun[4,3] & Jeffrey D. Brawn[5+]

[1] Program in Ecology, Evolution and Conservation Biology, University of Illinois at Urbana-Champaign, Urbana IL, 61801, USA
[2] Department of Evolution, Ecology, and Behavior, University of Illinois at Urbana-Champaign, Urbana IL, 61801, USA
[3] Behavior, Ecology, Evolution, and Systematics Program, University of Maryland, College Park, MD 20742, USA
[4] Department of Vertebrate Zoology, National Museum of Natural History, Smithsonian Institution, Washington, DC 20013, USA
[5] Department of Natural Resources, University of Illinois at Urbana-Champaign (UIUC), Urbana IL, 61801, USA
Corresponding author contact details
*kiralong778@gmail.com and [+]jbrawn@illinois.edu

Abstract

Hybrid zones are dynamic systems where natural selection, sexual selection and other evolutionary forces can act on reshuffled combinations of two distinct genomes. The movement of hybrid zones, individual traits, or both are of particular interest for understanding diversification processes. In a hybrid zone involving two lek-breeding birds (genus *Manacus*), secondary sexual plumage traits of *M. vitellinus,* especially bright yellow collars and olive bellies, have introgressed asymmetrically ~50 km across the genomic center of the zone into populations of *M. candei*. Males with yellow collars are preferred by females and are more aggressive than parental *M. candei*, suggesting that sexual selection was responsible for the introgression of male traits. To assess the spatial and temporal dynamics of this hybrid zone, we carried out a longitudinal reassessment using historical (1989 - 1994) and contemporary (2017 - 2020) transect samples to survey both morphological and genetic variation. Genome-scale SNP data and several male phenotypic traits show that the genomic center of the zone has remained spatially stable, whereas the olive belly color of male *vitellinus* has continued to introgress over time, suggesting that sexual selection may be an ongoing evolutionary force in this system.

Keywords

Manakin, RADseq, clines, hybridization, population genomics, sexual selection

Introduction

Hybridization is pervasive in nature and a key contributor to speciation and diversification processes (Abbott et al., 2013). For example, the study of hybrid zones is fundamental for understanding how species originate from diverging populations that may still be experiencing some degree of gene flow. We can observe a number of speciation and diversification processes in hybrid zones, including barriers to admixture developing through reinforcement (Coyne & Orr, 2004; Roberts & Mendelson, 2020), reproductive barriers breaking down allowing fusion between hybridizing species (Kearns et al., 2018; Seehausen, Alphen, & Witte, 1997), entirely new species arising through hybrid speciation (Gross & Rieseberg, 2005), and stable hybrid zones remaining in stasis for an indefinite period of time (Pinto, Titus-McQuillan, Daza, & Gamble, 2019; S. Wang, Rohwer, Delmore, & Irwin, 2019).

The movement or stability of hybrid zones is influenced by many different evolutionary factors. Moving hybrid zones are observed in a wide variety of taxa and can even move many kilometers in a single year, especially if one parental species has a selective or competitive advantage over the other species (Dasmahapatra et al., 2002; Harr & Price, 2014; Metzler, Knief, Peñalba, & Wolf, 2021; Reudink, Mech, Mullen, & Curry, 2007; Taylor et al., 2014; N. Wang et al., 2014; Wielstra, Burke, Butlin, & Arntzen, 2017; Zohren et al., 2016). Conversely, prolonged spatial stability is often seen in "tension zones" (Barton & Hewitt, 1985) where hybrids have lower fitness than parentals and the zones are localized in specific regions coinciding with population density troughs or ecological transition zones (Barton & Hewitt, 1985; Rosser, Dasmahapatra, & Mallet, 2014; Ruegg, 2008; Smith, Hale, Kearney, Austin, & Melville, 2013). Consequently, hybrid zones are dynamic systems, and their mobility or stasis may change over time along with changing evolutionary forces (Engebretsen, Barrow, Rittmeyer, Brown, & Lemmon, 2016; S. Wang et al., 2019).

Moreover, hybrid zones can involve conflicting evolutionary forces, such as sexual selection and natural selection, where selection for the traits of one form can be opposed by generalized selection against hybrids. The outcome of these pressures over time and space is a topic of active investigation (Buggs, 2007; Wielstra, 2019; Yang et al., 2022). Characterizing changes in hybrid zones over time can elucidate how species boundaries may go through periods of flux and allow us to capture the dynamics of evolution within these hybridizing populations.

Genome-scale analyses now provide the power to parse evolutionary change in unprecedented detail, revealing cryptic gene flow, demographic and selective history, and the genetic underpinnings of key traits in speciation and adaptation (Abbott, Barton, & Good, 2016; Moran et al., 2021; Payseur & Rieseberg, 2016; Taylor & Larson, 2019). For example, evidence of the prevalence of gene flow during speciation has expanded dramatically with advances in genome sequencing (Chan et al., 2020; Trigo et al., 2013), highlighting the importance of understanding incompatibilities and cryptic gene flow between diverging lineages. Additionally, modern genomics allows for the detailed categorization of hybrid zone movement in real time and tracking trait introgression down to the individual genes responsible for selected traits (Billerman, Cicero, Bowie, & Carling, 2019; Ottenburghs et al., 2017; Semenov et al., 2021; Wielstra, 2019).

We investigated a hybrid zone between golden-collared manakins (*Manacus vitellinus*) and white-collared manakins (*Manacus candei*) in western Panama. Both are lek breeding species, where females are choosy and males compete for mating opportunities by performing elaborate displays (Day et al., 2021; Kirwan & Green, 2011), leading to strong sexual selection on male traits (Snow, 2004). This hybrid zone was first characterized nearly 30 years ago, using morphological and genetic traits (Parsons, Olson, & Braun, 1993). Male collar and belly color transition across this hybrid zone from a golden yellow throat and olive belly in the golden-collared manakin to a white throat and yellow belly in the white-collared manakin (Fig. 1) (Brumfield, Jernigan, McDonald, & Braun, 2001; Parsons et al., 1993). The phenotypic transition for collar color occurred at the Río Changuinola, the largest river in the region, where birds on one side of the river had yellow collars and birds on the other side had white collars (Parsons et al., 1993). This phenotypic transition was displaced by about 50 km from the genetic cline centers (Brumfield et al., 2001). A similarly displaced transition was observed for male belly color, although that cline was not as sharp as the collar color cline (Brumfield et al., 2001; Parsons et al., 1993). This hybrid zone thus displayed unusual asymmetric introgression of two secondary sexual plumage traits of males. Moreover, assays of male aggression (McDonald, Clay, Brumfield, & Braun, 2001) and female choice (Stein & Uy, 2006b) indicated that yellow collars are favored over white collars, suggesting that sexual selection was responsible for collar color introgression. Belly color was correlated with collar color and thus may be directly or indirectly under sexual selection as well.

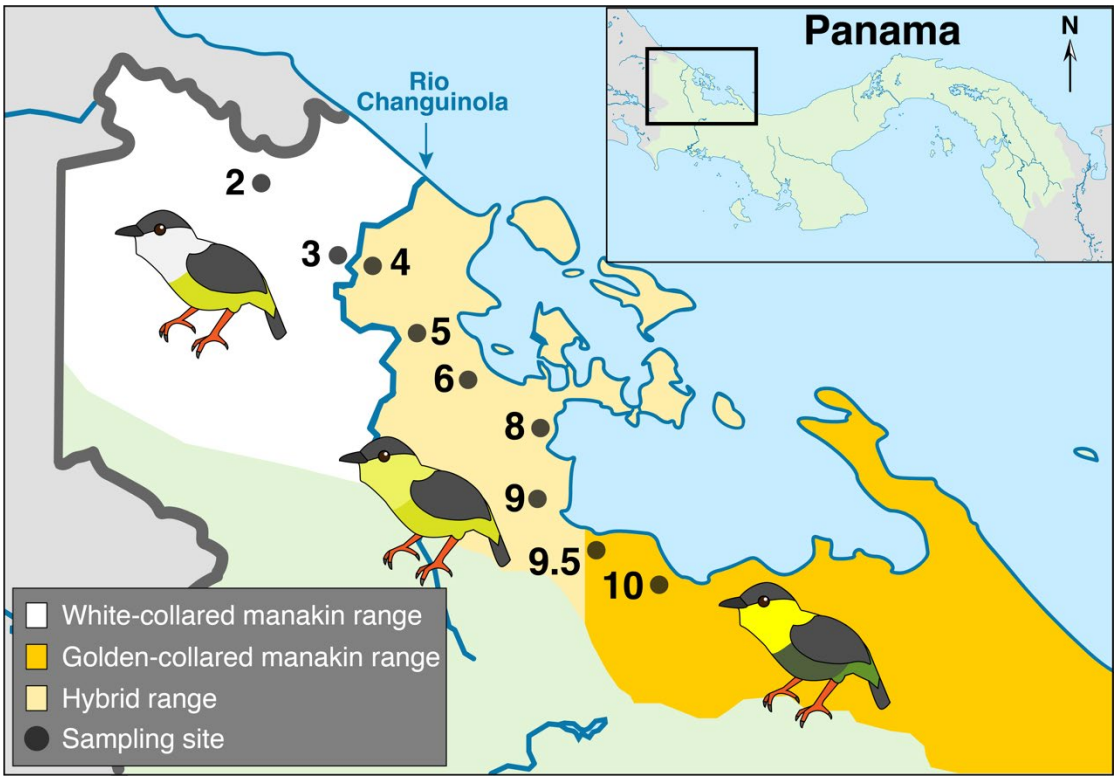

Figure 1. Map of the *Manacus* hybrid zone in Bocas del Toro, Panama. Dots represent sampling sites, numbered according to the system used in Brumfield et al. (2001). The shaded regions denote the approximate ranges of each parental species and hybrids in Panama based on the historical sampling. The cartoon birds illustrate the major phenotypic difference between the parental species and hybrid populations. The Río Changuinola is the largest river in the region, and it separates yellow-collared males on one side of the river from white-collared males on the other.

We aim to understand the spatial and temporal dynamics of this hybrid zone and the evolutionary forces that drive them. Here, we report the results of a longitudinal reassessment of morphological and genetic variation across the hybrid zone using a newly collected set of contemporary (2017 - 2020) samples that closely replicates the historical (1989 - 1994) transect. We categorized the genetic structure and admixture of the hybrid zone in both the historical and contemporary transects using a genome-wide set of single nucleotide polymorphism (SNP) markers derived from Restriction site-Associated DNA sequencing (RADseq). We also examined cline structure at both time points for previously identified male phenotypic traits of interest to look for evidence of cline movement and track introgressing traits. Overall, we ask whether this hybrid zone remained stable over time or whether we could find evidence of change in the years since it was first studied.

Methods

Study species and sampling sites

Manacus vitellinus and *M. candei* (Pipridae) are frugivorous birds that inhabit the understory of secondary forest or forest edge. *M. vitellinus* occurs from northern Colombia to Panama while *M. candei* ranges from southern Mexico to western Panama. For our historical dataset, we used many of the same specimens from the core transect collections of Parsons et al. (1993), Brumfield et al. (2001), Yuri et al. (2009), and Parchman et al. (2013). We then revisited the same sampling sites to collect contemporary samples. We replicated the core transect sampling design of Brumfield et al. (2001) as closely as possible, given land use changes in the intervening years between sample collection in 1989-1994 and 2017-2020. We sampled *Manacus* populations at 9 distinct sites in Bocas del Toro, Panama, located an average of 11.56 km apart (Fig. 1). We used site numbers corresponding directly to the numbering scheme used in Brumfield et al. (2001). Sampling site 9.5 (Miramar), located between sites 9 and 10, was added to the contemporary dataset and did not have previous historical transect data. We chose to focus our sampling within the active hybrid zone area, so sampling sites outside the province of Bocas del Toro were excluded, along with site 7 which deviated the farthest from the transect line. The 9 sampling sites represent two populations of *M. candei*, two populations of *M. vitellinus*, and 5 populations of hybrids in the known transition zone (Fig. 1, Table 1).

Table 1. Sampling sites and number of sequenced individuals retained for genetic analyses after quality filtering.

Sampling Site Number	Location Name	Distance from Site 10 (km)	Putative Hybrid Status	Historical N	Contemporary N
2	San San Drury	92.50	*M. candei*	31	49
3	El Silencio	79.00	*M. candei*	19	26
4	Finca Cuatro	71.25	Hybrid	18	24
5	Río Oeste	48.50	Hybrid	17	20
6	Quebrada Pastores	42.50	Hybrid	4	24
8	Río Uyama	29.50	Hybrid	22	27
9	Palma Real	20.75	Hybrid	23	65
9.5	Miramar	8.44	*M. vitellinus*	NA	30
10	Rambala	0.00	*M. vitellinus*	18	53

Field and museum data collection

We used 36mm mesh “ATX” type mist nets on leks to capture individuals. Each bird was given a numbered aluminum band and a combination of plastic colored leg bands to facilitate

individual identification. Birds were examined to determine age and sex using field observations of definitive adult male plumage and the presence of a brood patch for reproductive females. Non-breeding females and juvenile males were sexed using a molecular sexing protocol (see below). We collected blood samples (<100 μL) in glass capillary tubes from all individuals by puncturing the brachial vein. Blood was stored in Longmire's lysis buffer (Longmire, Maltbie, & Baker, 1997) and kept frozen to preserve long-term DNA quality. From males with definitive adult plumage, we measured beard length (measured as the longest feather directly below the front of the eye), epaulet width (measured as the widest point of the white or yellow coverts from the bend of the folded wing to the posterior edge of the white or yellow epaulet feathers), and tail length (measured as the longest feather in the tail).

We characterized male plumage colors using Ocean Insight reflectance spectrophotometers (USB2000+ in 2017 and FLAME-S-UV-VIS-ES in 2018-2022). Both spectrophotometers used a PX-2 pulsed xenon lamp (Ocean Insight). We used a fiber optic probe fitted with a plastic probe holder and took the feather color reads at a 90° angle. The probe holder minimized the ambient light in reflectance measurements and maintained the same distance between the probe and the feathers for each read. The percent reflectance across all wavelengths was measured relative to a pure white reflecting standard (WS-1-SL Diffuse Reflectance Std, Spectralon) as 100% reflectance and a 0% dark standard. The white standard was fitted with a plastic holder that kept the probe from directly touching the white substrate of the standard, keeping the white standard clean and free of discolorations. Due to the added distance between the probe holder and the white standard substrate, we calibrated our measurements to account for the drop in reflectance from this gap, which would be present evenly across the entire spectrum on each spectrophotometer. We adjusted the spectral curve values using a 0.7 and 0.5 multiplier for the USB2000+ and FLAME-S-UV-VIS-ES spectrophotometers, respectively, based on the percent drop in white reflectance as measured on both spectrophotometers following the calibration methods of Cook et al. (2013), Kelly et al. (2012), and Troy Murphy personal communication).

The reflectance data for the contemporary birds were taken on live birds in the field, while the reflectance data for the historical specimens were measured from museum skins at the Smithsonian National Museum of Natural History (NMNH) using the FLAME-S-UV-VIS-ES spectrophotometer. We took reflectance spectra of definitive male collar and belly plumage color

near the center of the throat or belly on each bird. Five spectra were taken for each plumage patch, repositioning the probe between each read and averaging across spectra for each bird. Following Brumfield et al (2001), we used the average adjusted reflectance at 490 nm and 665 nm to represent collar color and belly color respectively, because these wavelengths had the greatest differences in mean reflectance between the two parental samples. Outlier readings beyond two standard deviations (SDs) away from the mean for any individual were removed from the dataset. We used the average percent reflectance at each wavelength for geographic cline analysis.

All protocols involving live birds were reviewed and approved by the Illinois Animal Care and Use Committee and the Smithsonian Tropical Research Institute Animal Care and Use Committee (Illinois IACUC numbers: 15234 & 18239; STRI ACUC numbers: 2016-0301-2019 & 2019-0115-2022).

RADseq library preparation and genotype calling

DNAs from the contemporary 2017-2020 samples were extracted from whole blood using the animal tissue protocol on a Gene Prep automated extractor (Autogen), which involves Proteinase K digestion, phenol extraction, and alcohol precipitation. DNA concentrations were determined using a Quant-iT™ dsDNA Broad-Range Assay Kit (Thermo Fisher Scientific) on a SpectraMax® iD3 plate reader running SoftMax® Pro 7 software. DNA stocks for the historical 1989-1994 samples were available from previous studies (Brumfield et al., 2001; Parsons et al., 1993). All samples are deposited at the National Museum of Natural History, Smithsonian Institution, in Washington, D.C. DNAs from individuals of unknown sex were run in an avian polymerase chain reaction (PCR) molecular sexing protocol (Fridolfsson & Ellegren, 1999). Briefly, we made a master mix using the primers 2550F = 5'-GTT ACT GAT TCG TCT ACG AGA-3' and 2718R = 5'-ATT GAA ATG ATC CAG TGC TTG-3' and TaKaRa ExTaq DNA Polymerase (Takara Bio USA, Inc). We ran the samples for 31 cycles and ran the PCR product on a 2% agarose gel.

Six single-digest *SbfI* RADseq libraries were prepared using the protocols described in Baird et al. (2008) and Etter et al. (2011). After diluting all samples in the library to the same concentration, 600-800 ng of genomic DNA per-sample (depending on the library, see Table S1, Table S2) was digested using the *SbfI*-HF enzyme (New England Biolabs). Custom P1 adapters

containing unique 7-bp barcodes (Hohenlohe, Bassham, Currey, & Cresko, 2012) were ligated to each individual sample with T4 ligase (New England Biolabs). The DNA from all uniquely barcoded individuals in a library was pooled at equimolar concentration, and 1500 ng of total DNA was then sheared using Covaris (Covaris, Inc.), or Qsonica (Qsonica LLC) sonicators and size selected for 300-600 bp inserts using AMPure XP beads (Beckman Coulter). The sheared DNA was end-repaired and ligated to custom P2 adapters. The P2-ligated DNA was then amplified for 12 rounds of PCR using custom RAD primers (Hohenlohe et al., 2012) and cleaned with 0.8X AMPure XP beads (Beckman Coulter). The final libraries were sequenced either on an Illumina HiSeq 4000 or an Illumina NovaSeq 6000 to generate 2×150 bp reads (Table S2).

In total, 593 samples were processed, which included 542 unique individuals and 51 samples sequenced in duplicate to ameliorate low coverage. A breakdown of the detailed sequencing information per-library is provided in Table S2. Using the *Stacks* software version 2.60 (Rochette, Rivera-Colón, & Catchen, 2019), raw reads were filtered with `process_radtags` to remove reads with low quality (`-q`) and uncalled bases (`-c`), rescue ambiguous barcodes (`-r`), and demultiplex samples based on their unique barcode (`-b`). For each library, we retained between 668 million to 1.6 billion reads (Table S2).

The processed reads for all 593 sequenced samples were mapped to the *M. vitellinus* reference assembly (NCBI Refseq Accession: GCF_001715985.3) using *BWA* `mem` version 0.1.17 (H. Li & Durbin, 2009; Heng Li, 2013) with default parameters. Alignments were processed and sorted using *SAMtools* version 1.7 `view` and `sort` (H. Li et al., 2009). RAD loci assembly and genotyping from the processed alignments was done with the *Stacks* `gstacks` module version 2.60 (Rochette et al., 2019), where we removed PCR duplicates (`--rm-pcr-duplicates`). In total, we assembled 426,521 raw RAD loci with an average non-redundant coverage of 14.0× (SD 6.9×). To provide a baseline level filtering of missing data, we ran the *Stacks* `populations` module on all samples with an average per-locus coverage at 6× or higher, requiring a minimum minor allele count of 3 (`--mac 3`), requiring a locus to be present in at least 80% of samples per population (i.e., sampling sites) (`-r 0.80`), and be in all 9 populations (`-p 9`). Additionally, we used the `--hwe` flag to calculate differences between the observed and expected genotype frequencies under Hardy-Weinberg equilibrium (HWE) for each population. This filtered run kept 77,551 loci and 584,680 variant sites across 470 individuals (Table 1). This `populations`

run is hereafter referred to as the "master run" and its output was used to create all whitelists of loci/SNPs for downstream analyses.

Population structure analysis

We used *ADMIXTURE* (Alexander, Novembre, & Lange, 2009) to assess population genetic structure in both the historical and contemporary datasets. Using a custom Python script, we first created a whitelist of 10,000 SNPs sampled from our master `populations` run. First, we filtered the data from the master run for SNPs with a minimum allele frequency (MAF) of 1% and in HWE in all populations, and selected a single, randomly chosen SNP at each locus. From this filtered subset, the script then randomly selects 10,000 sites to generate a final whitelist. For each dataset, we reran the *Stacks* `populations` module, supplying the whitelist and exporting genotypes in the *PLINK* (`--plink`) and *GENEPOP* (`--genepop`) format. The resulting `.ped` files were converted to binary `.bed` files using *PLINK* version 1.90b6.25 (Chang et al., 2015) and *ADMIXTURE* version 1.3.0 was run separately on the historical and contemporary datasets for population cluster (K) values 1-9. To find an optimal value for the number of population clusters (K), we followed the *ADMIXTURE* documentation by plotting the cross validation (CV) error for each K value. To corroborate the results of *ADMIXTURE* using an ordination method instead of a clustering method, we ran a principal component analysis (PCA) using the same whitelisted SNP dataset described above in the *ADMIXTURE* analysis. We ran the PCA in *adegenet* version 2.1.7, an *R* package for multivariate analysis of genetic markers (Jombart, 2008; Jombart & Ahmed, 2011). The *ADMIXTURE* and PCA results were plotted in *R* version 4.2.1 (R Core Team, 2022).

Hybrid index

A hybrid index was calculated for each of 470 individuals across historical and contemporary datasets using the *R* package *gghybrid* (version 1.0.0) (Bailey, 2020), which uses a Bayesian Markov chain Monte Carlo (MCMC) method for estimating the hybrid index. First, using the same whitelist of 10,000 loci as the *ADMIXTURE* analysis, we re-ran `populations` to export the genotypes in the *STRUCTURE* format (`--structure`). When importing the genotypes to *gghybrid*, we filtered variant sites based on the parental allele frequencies at sampling site 2 (*M. candei*) and site 10 (*M. vitellinus*), requiring a MAF of 10% and unequal frequencies between the two parental sites (default in *gghybrid*). *gghybrid* assigns the designated parental populations

as 0 or 1 in the index, which we designated as sampling site 2 and site 10, respectively. This analysis was performed separately for the historical and contemporary datasets. We recorded the mean hybrid index value for each individual and used the mean for each sampling site in downstream analyses.

Geographic clines

For the geographic clines, we reran the same custom Python script to filter the master run to obtain all sites that were in HWE in each of the 9 populations and only a single SNP per locus, retaining a total of 72,506 loci. Sites in HWE were used for the geographic cline analysis because sites that drastically depart from equilibrium could bias cline fittings (Derryberry, Derryberry, Maley, & Brumfield, 2014; Macholán et al., 2008, 2007; Phillips, Baird, & Moritz, 2004). All geographic cline analyses were repeated with and without the newly added sampling site 9.5. With the new 72.5K SNP whitelist, we re-ran the *Stacks* `populations` module to export genotypes in the *HZAR* format (`--hzar`). *HZAR* is an *R* package designed to fit geographic clines to one-dimensional transect data in hybrid zones using the Metropolis-Hastings Markov chain Monte Carlo algorithm (Derryberry et al., 2014). We wrote a custom *R* script to parallelize *HZAR* (version 0.2-5), allowing us to efficiently run the analysis independently for each selected SNP. Of the 72.5K whitelisted markers, we removed sites that were invariant in either the contemporary or historical datasets, ensuring that only sites that were variant in both datasets were run in *HZAR*. In total, we retained 68,684 and 63,444 SNPs in the contemporary and historical datasets, respectively. For each SNP in the historical and contemporary datasets, we ran *HZAR* using four of the 16 available cline models (as originally described by (Szymura & Barton, 1986, 1991)) to maintain consistency with the analyses performed by Brumfield et al. (2001):1) a model with the observed minimum (p_{min}) and maximum (p_{max}) allele frequencies and without fitting exponential decay curves for the cline tails, 2) estimated p_{min} and p_{max} without fitted exponential decay curves, 3) estimated p_{min} and p_{max} with fitting decay curves to both cline tails, and 4) a null model without fit for either allele frequency or cline tails. For each model, we ran 3 independent chains, composed of three dependent model fit requests, each of length 100,000 and with 10,000 burn-in generations. The best fit model was selected using Akaike Information Criterion (AICc). We then extracted the estimated cline width (1/maximum slope) and cline center values with 95% Bayesian Credibility Intervals (CI) for the best model of each cline, along

with the maximum likelihood cline generated by the best model. We removed sites that were assigned null models (i.e., indicating that the SNP was not clinal and thus contained null values for the cline center and width). In the historical and contemporary datasets, there were 11,925 and 8,254 sites, respectively, that were non-clinal and thus were assigned null models. We used a custom Python script to combine the cline parameter outputs into a single file and to select clines at loci that were present in both the historical and contemporary datasets, leaving 48,216 clines that passed all the above filters for direct comparison. For visualizing overall cline structure, we removed SNPs with credibility intervals for cline centers greater than the average distance between sampling sites (11.56 km), to better localize which site the cline centers were associated with and thus also removing uninformative clines with credibility intervals wider than the entire hybrid zone (92.5 km between sites 10 and 2). For direct comparison between the historical and contemporary transect, we retained 4,135 sites still present in both datasets following filtering. The distribution of all cline centers without the CI filtering is shown in Fig. S1, showing the same overall distribution as the filtered data.

We also ran *HZAR* on five phenotypic traits of males known to differ between *M. vitellinus* and *M. candei*: beard length, epaulet width, tail length, collar color, and belly color. We ran three morphological cline models: 1) a model with the observed morphological data ("fixed") and without fitting exponential decay curves for the cline tails, 2) estimated "free" without fitted exponential decay curves, 3) estimated "free" and fitting decay curves to both cline tails. After running each model three times with a chain length of 100,000, and burn-in of 10,000, the best fit model was selected using AICc. The cline analyses for the contemporary dataset was performed both with and without data for site 9.5 to directly match the historical dataset. For any phenotypic traits that displayed substantial changes in cline center or width estimates, we further validated these results by running longer chain lengths of 1,000,000 and visually inspecting the MCMC trace plots. In addition to the five male phenotype clines, we ran a geographic cline on the genomic hybrid index calculated by *gghybrid,* to assess genome-wide movement of the hybrid zone. We calculated the mean hybrid index values in each sampling site for both the contemporary and historical datasets and analyzed them using *HZAR*. As with the SNP data, we obtained the best cline model and exported the associated center, width, and CI values. For both the phenotypic clines and hybrid index clines, we assessed whether the clines had moved based on whether the historical and contemporary CIs for the cline centers overlapped.

Results

Genome-wide patterns of genetic population structure are stable through time

We sampled 10,000 SNPs from 470 sequenced individuals spanning the historical and contemporary datasets. Overall, we found genetic population structure to be consistent over time at a genome-wide level. When we assessed admixture with two genetic clusters (K=2), individuals separated based on apparent parental species ancestry (Fig. 2). The genomic transition from *M. vitellinus* to *M. candei* was centered near site 9, with substantially admixed individuals present only at sites 8, 9 and 9.5. Although all birds in sites 4-8 closely resemble *vitellinus* phenotypically, their genomes are *candei*-like, aside from a few intermediate individuals at site 8.

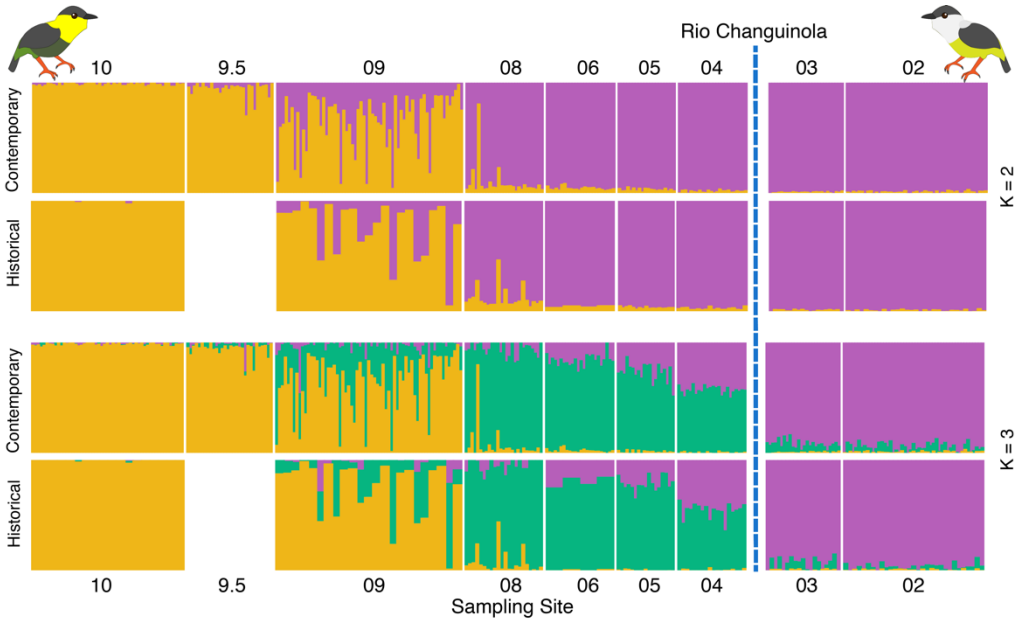

Figure 2. Admixture analysis of contemporary and historical manakin datasets based on 10,000 SNPs. Sampling site numbers are listed at the top and bottom of the figure with the *M. vitellinus* site 10 on the left and *M. candei* site 2 on the right. Site 9.5 was sampled for the contemporary but not the historical dataset. Each vertical bar represents one bird; width of contemporary and historical population blocks was equalized for ease of comparison. The dashed blue vertical line between sites 3 and 4 represents the Río Changuinola, marking the phenotypic transition of yellow to white collar plumage.

K=3 was the best fit model for both historical and contemporary datasets according to cross validation analyses (Table S3). With K=3, a third cluster separated hybrids with candei-like genomes east of the Río Changuinola (sites 4-9) from *M. candei* to the west (sites 2 and 3), highlighting the river as an important barrier to gene flow (Fig. 2). The largest variance in

admixture proportions is still seen in sampling site 9 in both time points. Patterns of admixture are consistent with K=2 and K=3 clustering for both the historical and contemporary transect samples, showing that overall admixture and genetic clustering in the hybrid zone is stable over the time period examined.

The PCA corroborated the admixture analysis. Individuals in the PCA group by sampling site and not by time, also implying temporal stability in genome-wide structure. The first principal component axis (PC1) separates individuals based on apparent parental ancestry, explaining 14.54% of SNP variance (Fig. 3A). We found a tight correlation between PC1 scores and genomic hybrid index, suggesting that the primary axis of SNP variation strongly corresponds with parental ancestry (Fig. 3B). Sampling site 9, again, showed the largest gradient and variation of all the sampling sites, spanning between the *M. vitellinus* parental cluster and the other hybrid sites. Additionally, parental *M. candei* sites 2 and 3, both to the west of the Río Changuinola, clustered tightly together and are separated from the rest of the hybrid sites along PC2; however, this axis only explains a small proportion of the observed variation (1.56%).

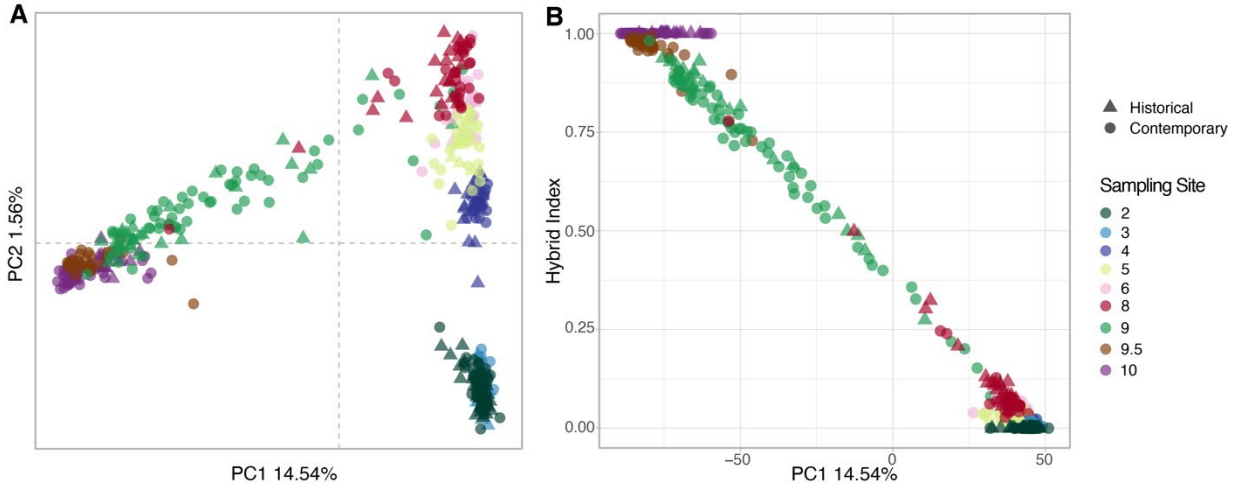

Figure 3. **A)** Principal component analysis based on 10,000 SNPs from contemporary and historical manakin datasets. **B)** Correlation between the first principal component and genomic hybrid index for sites 3-9.5 (Note that sites 2 and 10 were assigned values of 0 and 1 to construct the hybrid index).

Genomic hybrid index reflects stable patterns of parental ancestry

The hybrid indices were stable over time and showed no movement of the hybrid zone (Fig. 4). Birds sampled at sites 4-8 for both contemporary and historical transects possessed a minor amount of *M. vitellinus* ancestry in a majority *M. candei* genomic background, with one

notable exception in site 8 of a single individual with a hybrid index of 0.78 (Fig. 4A, Table S4). The contemporary samples from newly-assayed site 9.5 showed a majority *M. vitellinus* ancestry, with a mean hybrid index of 0.9470 (SD 0.0612). Hybrids from site 9 had the highest levels of variation in hybrid index in both the contemporary and historical datasets (Fig. 4A, Table S4). This result is consistent with the population level structure analyses above, showing that site 9 is consistently the most variable and admixed locality in the hybrid zone. Thus, the proportion of genome-wide parental ancestry in hybrid individuals appears stable over time at the population level.

To further assess hybrid zone movement, we derived geographic clines for the genomic hybrid index from the historical and contemporary transect datasets (Fig. 4B). The cline centers and cline widths for the two datasets were similar with overlapping credibility intervals (Table S5). The cline center credibility intervals from both datasets overlapped the location of hybrid sampling site 9, about 20.75 km from *M. vitellinus* parental site 10. Thus, the genomic center of the hybrid zone has remained stable over time near sampling site 9.

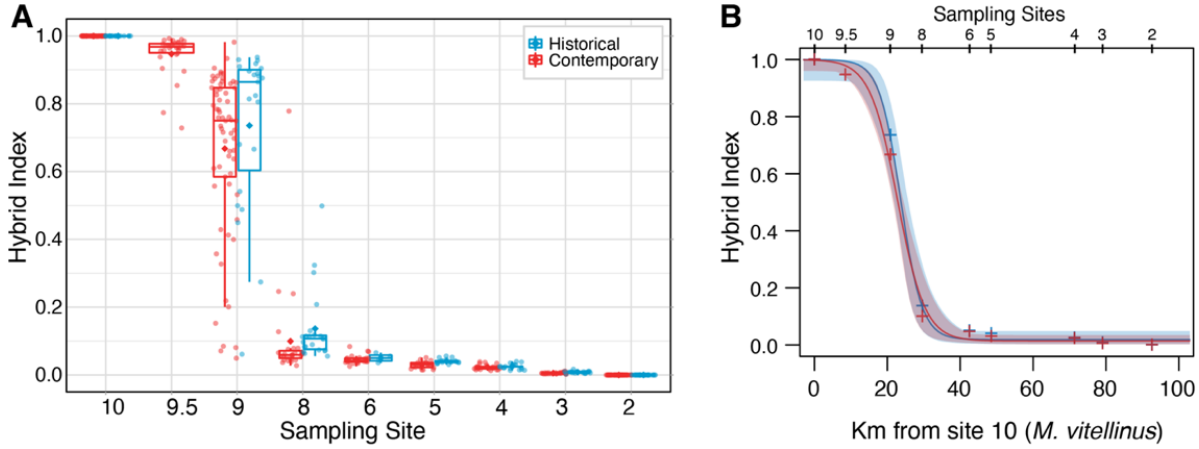

Figure 4. **A)** Boxplots showing the distribution of genomic hybrid index values of historical and contemporary transect samples. A hybrid index of 0 indicates complete *M. candei* ancestry (site 2) while a value of 1 indicates complete *M. vitellinus* ancestry (site 10). **B)** Geographic clines of the hybrid index and associated 95% credibility intervals, with the historical dataset in blue and contemporary in red. The top x-axis shows the location of the 9 sampling sites. The crosses denote the mean hybrid index at each site.

Stability of genome-wide geographic clines

Of 72,506 loci in the RADseq dataset, 4,135 contained SNPs that displayed clinal variation across the transect and passed all filters for cline center analysis. The clines from the historical samples had a median cline center at 23.37 km from site 10, the *M. vitellinus* parental

site (mean = 23.90 km, SD 3.55 km) (Fig. 5). The contemporary dataset had a median cline center at 22.28 km from site 10 (mean = 22.53 km, SD 3.22 km). These results are identical when population 9.5 is added to the contemporary dataset (Fig. S2). The widths of these 4,135 clines had a historical median of 7.33 km (mean = 7.51 km, SD 6.52 km) and contemporary median width of 10.38 km (mean = 11.25 km, SD 8.08 km) (Fig. S3). Only 25 (historical) and 22 (contemporary) cline centers were displaced beyond site 8 (29.5 km from site 10); however, 12 historical and 9 contemporary clines are displaced up to the Río Changuinola between sites 3 and 4, indicating a limited, but detectable, amount of genetic introgression up to the river. Overall, the genome-wide distribution of cline centers is stable between the two time points and supports site 9 as the genomic center of the *Manacus* hybrid zone.

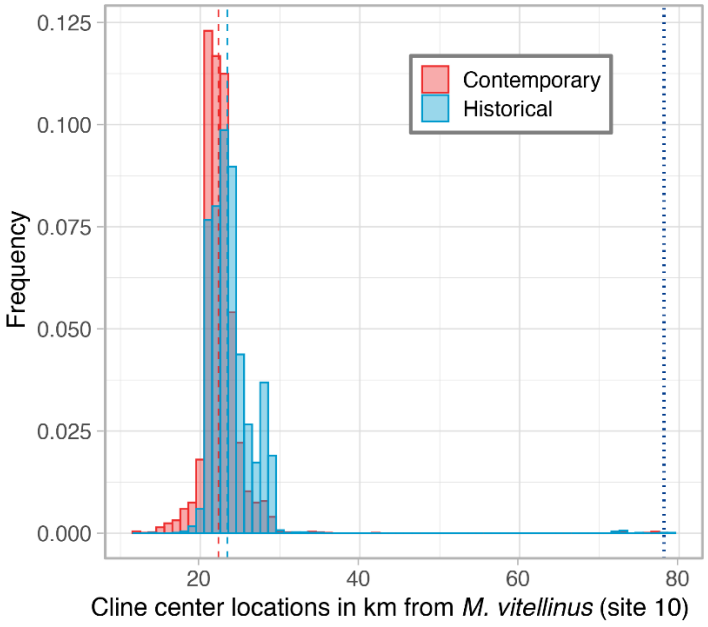

Figure 5. Histogram of estimated geographic cline center locations for 4,135 genome-wide SNPs present in both the contemporary and historical datasets with the additional site 9.5 included in the contemporary dataset. The dark blue dotted line denotes the Río Changuinola. The dashed lines represent the median cline center locations for the two datasets.

Introgression of plumage traits

In addition to the distribution of allele frequencies across space, we also fit sigmoid clines to the observed variation in five male plumage traits (beard length, epaulet width, tail length, collar color, and belly color) in both historical and contemporary transect samples (Table S6, Table S7). Clines for four plumage traits are similar in the historical and contemporary transects (Fig. 6A-D, Table S5), suggesting these traits are largely geographically stable through time.

Beard length and tail length cline centers lie near the genomic center of the hybrid zone (site 9) at ~23 km from sampling site 10, while the collar color cline centers lie more than 50 km further along the transect near the Río Changuinola (Fig. 6F). The CIs for beard length cline centers overlap between the contemporary and historical datasets; however, the CIs for cline widths do not overlap so it appears that the contemporary cline has widened by ~11 km (Table S5). This widening could indicate some degree of bidirectional introgression or relaxed selection on beard length, but we do not currently have further evidence to explain this change. Epaulet width is a shallow cline that spans the whole hybrid zone and does not exhibit a strong sigmoidal shape (Fig. 6B). Cline estimates for epaulet width were inconsistent across the analysis, with the best cline model switching between model I and III depending on the chain length and the addition of the contemporary sampling site 9.5 (Table S8). Given these results, we cannot accurately resolve whether this cline has changed over time.

In contrast, the olive belly coloration has introgressed further across this hybrid zone over the last 30 years (Fig. 6E, Table S5). The historical dataset has an estimated cline center for belly color at 71.31 km (95% CI 67.74 – 75.47 km) while the contemporary dataset has an estimated cline center at 80.47 km (95% CI 77.89 – 84.59 km). Based on the lack of overlap between the two comparisons, we conclude that this cline has moved about 9 km in the last 30 years. The cline for belly color also narrowed significantly, with an estimated historical width of 60.58 km (95% CI 50.98 – 72.46 km) compared to only 8.73 km (95% CI 1.55 – 17.02 km) for the contemporary dataset. The difference in the contemporary and historical belly color clines was consistent whether or not sampling site 9.5 was included in the analyses (Table S5). Thus, the belly color cline has shifted to the Río Changuinola (Fig. 6F) and is now similar in position and width to the collar color cline.

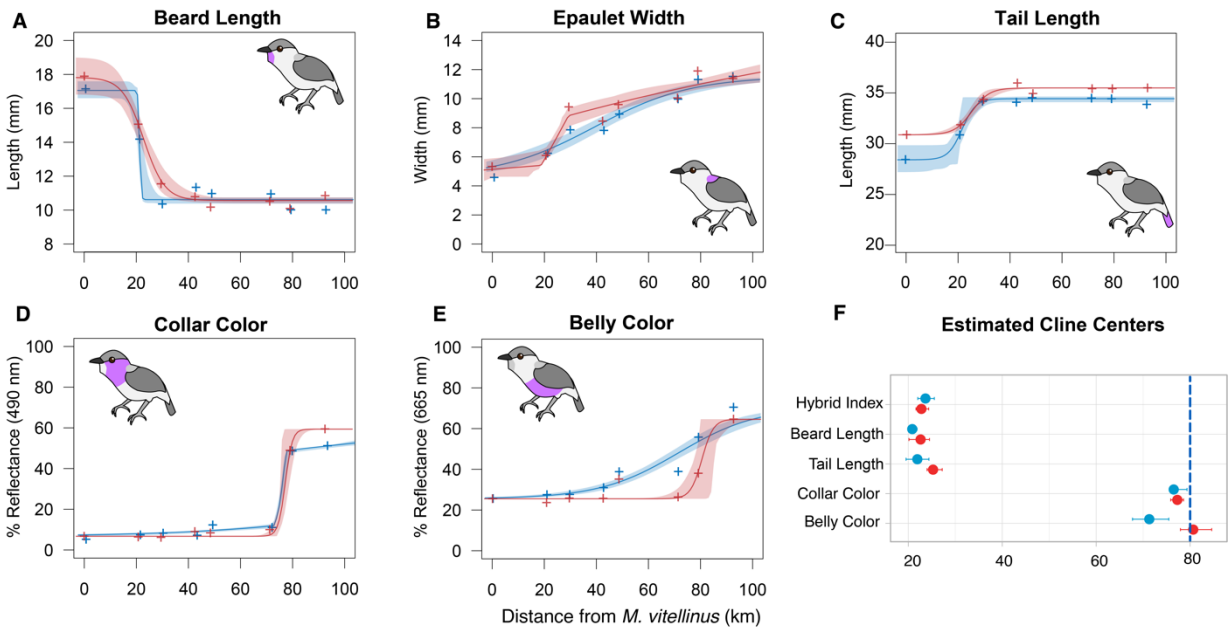

Figure 6. Contemporary and historical clines estimated from manakin phenotypic data across 8 sampling sites. For all panels, blue denotes the historical dataset, red the contemporary dataset, and all x-axes are in kilometers from the parental *M. vitellinus* (site 10). Crosses in A-E represent the average value of the phenotypic trait of interest in each sampling site. Shaded regions represent 95% credibility intervals for each cline. Magenta patches on the manakin cartoons highlight the plumage patches measured for each trait. (F) Location along the transect of the maximum likelihood estimated cline center (dot) with 95% credibility intervals (horizontal bars) for the traits of interest. Hybrid index values pertain to the genomic hybrid index cline shown in Figure 4. The vertical blue dashed line represents the location of the Río Changuinola.

Discussion

This hybrid zone between the golden-collared manakin and the white-collared manakin is one of the few hybrid zones to show asymmetrical introgression of a male secondary sexual trait. We found clear evidence that the genomic transition of this hybrid zone and several phenotypic clines have remained spatially stable over the span of ~25-30 years. Moreover, we also found evidence that belly plumage coloration, a male secondary sexual trait, has moved since the initial sampling. This interplay between genomic stasis and introgression of key male plumage traits highlights the likely importance of sexual selection on the temporal dynamics of hybrid zones. Although the possibility of direct sexual selection on belly color has not been formally tested, its expression and introgression is correlated with yellow male collar color, which has been shown to be under positive sexual selection in this hybrid zone (McDonald et al., 2001; Stein & Uy, 2006b, 2006a).

Asymmetrical introgression in avian tension zones

Previous studies categorizing the *Manacus* hybrid zone phenotypically and genetically found evidence of asymmetrical introgression of male *M. vitellinus* plumage traits, yellow collar color and olive belly color, into populations dominated genetically by *M. candei* (Brumfield et al., 2001; Parchman et al., 2013; Parsons et al., 1993). Yet, despite this introgression, the *Manacus* hybrid zone remains narrow over time, consistent with previous *Manacus* studies which found 6 out of 7 genetic markers had cline widths of less than 11 km (Brumfield et al., 2001). Additionally, our genomic hybrid index and admixture analysis corroborate the previous studies (Brumfield et al., 2001; Parchman et al., 2013; Parsons et al., 1993), finding that sampling sites 4 - 8 are majority *M. candei*-like and that site 9 is the genomic hybrid center of the hybrid zone.

Studies of other avian hybrid zones also report asymmetrical introgression within narrow hybrid zones (e.g., northern flickers (Aguillon & Rohwer, 2022); red-backed fairy-wrens (Baldassarre, White, Karubian, & Webster, 2014); long-tailed finch (Griffith & Hooper, 2017); wagtails (Semenov et al., 2021); jacanas (Lipshutz et al., 2019); tanagers (Morales-Rozo, Tenorio, Carling, & Cadena, 2017)). Many of these hybrid zone studies posit that movement may be controlled by changes in the environment (Aguillon & Rohwer, 2022; Carling & Brumfield, 2008; Carling & Zuckerberg, 2011; Walsh, Billerman, Rohwer, Butcher, & Lovette, 2020), or climate change (Taylor et al., 2014); however, sexual selection appears to play a more important role in the *Manacus* hybrid zone. Our findings better align with other hybrid zones that display traits under selection by either intersexual (mate choice) or intrasexual (competition for access to mates) (Baldassarre et al., 2014; Lipshutz et al., 2019; Yang et al., 2018), which show a trait under sexual selection displaced from the genomic hybrid center. The *Manacus* hybrid zone is a prime example of sexual selection driving key diagnostic traits across species boundaries; however, not all displaced clines represent ongoing introgression (Semenov et al., 2021). As such, reassessing hybrid zones with asymmetrical introgression over multiple time points helps to clarify which traits have ongoing introgression.

Barriers to gene flow despite positive selection

Male collar color displayed nearly identical clines in the contemporary and historical datasets; specifically, a sharp transition in collar color from yellow to white occurring at the Río Changuinola (Fig. 1). Collar color likely introgressed through positive sexual selection mediated

by female choice (Stein & Uy, 2006b), male aggression (McDonald et al., 2001), or both. If positive sexual selection is still operative, as it appears to be for belly color, collar color should continue to spread. However, yellow collar plumage appears to be "stuck" at the river, displaced by more than 50 km from the genomic transition, consistent with previous studies (Brumfield et al., 2001; Parchman et al., 2013; Parsons et al., 1993). Thus, the Río Changuinola appears to present a limit to collar color introgression, either by acting as a barrier to gene flow or marking a transition in another relevant evolutionary factor (Bennett, Lim, & Braun, 2021). Belly color introgression may prove to be similarly limited at the river.

Rivers have been shown as effective barriers to dispersal in tropical birds (Haffer, 1997; Naka, Bechtoldt, Henriques, & Brumfield, 2012; Naka, Costa, Lima, & Claramunt, 2022) and other taxa, e.g., frogs (Fouquet et al. 2012), primates (Fordham, Shanee, & Peck, 2020), butterflies (Rosser, Shirai, Dasmahapatra, Mallet, & Freitas, 2021). However, the extent that a river, or any geographic barrier, serves to reduce gene flow likely depends on the dispersal mode or capability of the species of interest (Claramunt, Derryberry, Remsen, & Brumfield, 2012; Claramunt, Hong, & Bravo, 2022; Naka et al., 2022; Nazareno, Knowles, Dick, & Lohmann, 2021). Additionally, dispersal is highly predictive of hybrid zone widths (McEntee, Burleigh, & Singhal, 2020). The golden-collared manakin is capable of flying substantial distances over open water (Moore, Robinson, Lovette, & Robinson, 2008). Moreover, we observed radio-tagged females dispersing beyond a kilometer from the lek where they were tagged, and in one case a female *M. vitellinus* individual was tracked flying about 100m over open cattle pasture to a neighboring stand of trees to forage before flying back to the lek in an isolated forest patch (KML personal observation). Additionally, *Manacus* manakins are secondary forest specialists and most leks in our study area are along waterways or flanked by cacao plantations or cattle pastures. Thus, while the Río Changuinola seems to be acting as a barrier to gene flow given the location of the displaced clines, *Manacus* manakins are capable of crossing the river, and there have been a few cases recorded of yellow collared males on the west bank of the river (McDonald et al., 2001; Stein & Uy, 2006b, KML personal observation). Therefore, dispersal ability alone is insufficient to explain why clines under positive selection remain "stuck" at the Río Changuinola, instead of spreading further beyond the river. Further research is necessary to understand what other mechanisms may be playing a role in stalling introgression at the Río Changuinola (Bennett et al., 2021).

Melanization as a candidate for selection

Similar to the yellow collar in *M. vitellinus*, olive belly color introgressed from *M. vitellinus* into *M. candei* and is displaced from the genomic center of the hybrid zone. Here, we find evidence that belly color has continued to introgress and its cline center has moved ~9 km over the last 30 years, leading to a current phenotypic transition at the Río Changuinola. Given an estimated generation length of ~2.5 years (averaged from estimates of *M. candei* and *M. vitellinus* from Bird et al. (2020)), this means that in about 12 generations belly color has introgressed about 0.7 km per generation. In addition, belly color has higher variation than collar color, a pattern also noted by Brumfield et al. (2001), with males present at the same lek in sites 4 or 5 having yellow, green, or intermixed belly coloration. Moreover, when visually comparing the historical skins from sampling site 4 (just east of the Río Changuinola) versus living birds, the bellies of birds at site 4 today are clearly greener than they were 30 years ago (KML personal observation).

Several non-exclusive factors could explain selection for dark bellies in hybrid populations from natural or sexual selection. For natural selection, there could be an ecological or environmental advantage to having darker olive bellies. For sexual selection, both female choice and male-male competition have been implicated as important in lek-breeding systems and the *Manacus* system in particular. We propose a few hypotheses for sexual selection: 1) there is a sexual advantage of a yellow collar that is enhanced by contrast with a dark belly, so both introgress together, 2) females prefer olive bellies over yellow bellies independently from collar plumage, 3) males with olive bellies are more aggressive and could benefit from male-male competition. We expand on the male-male aggression/melanization hypothesis below.

The olive color in *Manacus* dark bellies is proposed to result from melanin deposition on yellow feathers (Bennett et al., 2021). Pathways controlling aggression and melanin production share some of the same upstream regulators (Ducrest et al. 2008), which has been proposed as an explanation for the observed pattern that animals with darker colorations tend to be more aggressive, especially in birds (Da Silva et al., 2013; de Zwaan, Barnes, & Martin, 2019; Ducrest et al., 2008; Mafli, Wakamatsu, & Roulin, 2011; Mateos-Gonzalez & Senar, 2012). Whether manakins with darker bellies are more aggressive remains to be tested directly, but two previous studies performed aggression assays on *Manacus* manakins based on hybrid status. McDonald et

al. (2001) found that hybrid males from the region of yellow plumage introgression were the most aggressive to the presentation of a mount, followed by *M. vitellinus* males, and lastly *M. candei* males. Stein and Uy (2006) performed a similar experiment and found no difference in aggression between yellow and white collared males; however, they worked in a different location along the upper Río Changuinola where the river is narrow and mixed leks with yellow and white collared birds are found.

If aggression in *Manacus* is influenced by melanization, then the difference in response of the manakins tested in the two previous studies could be explained by differences in the introgression of dark melanized bellies. Specifically, McDonald et al. (2001) tested yellow-collared males near sampling site 5, where belly color is typically darker than in leks along the upper Río Changuinola where Stein and Uy (2006) worked. Both studies focused on yellow-collared hybrids, but neither quantified the belly color of the birds tested. If aggression is linked to green bellies/increased melanization more so than yellow collars, their results may be reconcilable. Careful experiments that directly test female preference for olive bellies, male aggression trials with varying olive belly colors, as well as categorizing the genes and metabolic pathways responsible for melanization in this hybrid zone, will be necessary to tease apart the connection of introgressing olive bellies, melanization, male-male aggression, and the subsequent effect on hybrid zone dynamics.

Author Contributions

KML, MJB, and JDB conceived and designed the study. KML collected field data, made graphics, and wrote the original draft of the manuscript. KFPB contributed lab work and sequencing data. KML and AGRC performed lab work and analyzed the data. AGRC, KFPB, JMC, MJB, and JDB provided discussions and feedback on the text and analyses. All authors approved the final manuscript.

Acknowledgements

We thank the Smithsonian Tropical Research Institute, including Lil Camacho, Raineldo Urriola, and Isis Ochoa, for logistics and MiAmbiente for permitting. We thank Cesar Romero for logistics and hospitality, and our field assistants: Adolfo Muñoz, Ovidio Jaramillo, André Nguyen, Alexander Worm, Ivy Ciaburri, Olivia Ferrari, Elena Prado-Ragan, Vaughn Hage, Luis

Ramos Vazquez, and Evalynn Trumbo. We are grateful to the local families and communities who supported our work including, but not limited to, the Jimenez family, the Lezcano family, the Aguilar family, the López family, and the Teribe peoples and the Ngäbe-Buglé peoples. Thank you to the staff at the University of Illinois at Urbana-Champaign departments of Natural Resources and Environmental Sciences, Integrative Biology, and the Smithsonian's National Museum of Natural History, including Mary Faith Flores and Carrie Craig. Additionally, we thank Becky Fuller, Troy Murphy, Tom Parsons, Peri Bolton, and Karthik Yarlagadda for helpful discussions and advice on this manuscript. This project was supported by the NSF DGE 10-69157 IGERT to KML and AGRC, the USDA National Institute of Food and Agriculture, Hatch project 1026333 (ILLU-875-984), the Smithsonian Institution and a National Museum of Natural History Core grant to MJB.

Data Accessibility

DNA sequence datafiles will be available under the NCBI Bioproject PRJNA893627. Scripts for analyses and figures are available at https://github.com/kiralong.

Conflict of Interest

The authors declare no conflict of interest.

References

Abbott, R. J., Albach, D., Ansell, S., Arntzen, J. W., Baird, S. J. E., Bierne, N., … Zinner, D. (2013). Hybridization and speciation. *Journal of Evolutionary Biology*, *26*(2), 229–246. https://doi.org/10.1111/j.1420-9101.2012.02599.x

Abbott, R. J., Barton, N. H., & Good, J. M. (2016). Genomics of hybridization and its evolutionary consequences. *Molecular Ecology*, *25*(11), 2325–2332. https://doi.org/10.1111/mec.13685

Aguillon, S. M., & Rohwer, V. G. (2022). Revisiting a classic hybrid zone: Movement of the northern flicker hybrid zone in contemporary times. *Evolution*, *76*(5), 1082–1090. https://doi.org/10.1111/evo.14474

Alexander, D. H., Novembre, J., & Lange, K. (2009). Fast model-based estimation of ancestry in unrelated individuals. *Genome Research*, *19*(9), 1655–1664. https://doi.org/10.1101/gr.094052.109

Bailey, R. I. (2020). gghybrid: R package for evolutionary analysis of hybrids and hybrid zones. https://doi.org/10.5281/zenodo.3676499

Baird, N. A., Etter, P. D., Atwood, T. S., Currey, M. C., Shiver, A. L., Lewis, Z. A., … Johnson, E. A. (2008). Rapid SNP Discovery and Genetic Mapping Using Sequenced RAD Markers. *PLoS ONE*, *3*(10), e3376. https://doi.org/10.1371/journal.pone.0003376

Baldassarre, D. T., White, T. A., Karubian, J., & Webster, M. S. (2014). Genomic and morphological analysis of a semipermeable avian hybrid zone suggests asymmetrical introgression of a sexual signal. *Evolution*, *68*(9), 2644–2657. https://doi.org/10.1111/EVO.12457

Barton, N. H., & Hewitt, G. M. (1985). *Analysis of hybrid zones*. *Ann. Rev. Ecol. Syst* (Vol. 16). Retrieved from www.annualreviews.org

Bennett, K. F. P., Lim, H. C., & Braun, M. J. (2021). Sexual Selection and Introgression in Avian Hybrid Zones: Spotlight on Manacus. *Integrative and Comparative Biology*, *61*(4), 1291–1309. https://doi.org/10.1093/icb/icab135

Billerman, S. M., Cicero, C., Bowie, R. C. K., & Carling, M. D. (2019). Phenotypic and genetic introgression across a moving woodpecker hybrid zone. *Molecular Ecology*, *28*(7), 1692–1708. https://doi.org/10.1111/MEC.15043

Bird, J. P., Martin, R., Akçakaya, H. R., Gilroy, J., Burfield, I. J., Garnett, S. T., … Butchart, S. H. M. (2020). Generation lengths of the world's birds and their implications for extinction risk. *Conservation Biology*, *34*(5), 1252–1261. https://doi.org/10.1111/cobi.13486

Brumfield, R. T., Jernigan, R. W., McDonald, D. B., & Braun, M. J. (2001). Evolutionary implications of divergent clines in an avian (Manacus: aves) hybrid zone. *Evolution*, *55*(10), 2070–2087. https://doi.org/10.1111/j.0014-3820.2001.tb01322.x

Buggs, R. J. A. (2007). Empirical study of hybrid zone movement. *Heredity*, *99*(3), 301–312. https://doi.org/10.1038/sj.hdy.6800997

Carling, M. D., & Brumfield, R. T. (2008). Haldane's rule in an avian system: using cline theory and divergence population genetics to test for differential introgression of mitochondrial, autosomal, and sex-linked loci across the passerina bunting hybrid zone. *Evolution*, *62*(10), 2600–2615. https://doi.org/10.1111/J.1558-5646.2008.00477.X

Carling, M. D., & Zuckerberg, B. (2011). Spatio-temporal changes in the genetic structure of the Passerina bunting hybrid zone. *Molecular Ecology*, *20*(6), 1166–1175. https://doi.org/10.1111/j.1365-294X.2010.04987.x

Chan, K. O., Hutter, C. R., Wood, P. L., Grismer, L. L., Das, I., & Brown, R. M. (2020). Gene flow creates a mirage of cryptic species in a Southeast Asian spotted stream frog complex. *Molecular Ecology*, *29*(20), 3970–3987. https://doi.org/10.1111/mec.15603

Chang, C. C., Chow, C. C., Tellier, L. C. A. M., Vattikuti, S., Purcell, S. M., & Lee, J. J. (2015). Second-generation PLINK: Rising to the challenge of larger and richer datasets. *GigaScience*, *4*(1). https://doi.org/10.1186/S13742-015-0047-8

Claramunt, S., Derryberry, E. P., Remsen, J. V., & Brumfield, R. T. (2012). High dispersal ability inhibits speciation in a continental radiation of passerine birds. *Proceedings of the Royal Society B: Biological Sciences*, *279*(1733), 1567–1574. https://doi.org/10.1098/rspb.2011.1922

Claramunt, S., Hong, M., & Bravo, A. (2022). The effect of flight efficiency on gap-crossing ability in Amazonian forest birds. *Biotropica*, *54*(4), 860–868. https://doi.org/10.1111/btp.13109

Cook, E. G., Murphy, T. G., & Johnson, M. A. (2013). Colorful displays signal male quality in a tropical anole lizard. *Naturwissenschaften*, *100*(10), 993–996. https://doi.org/10.1007/s00114-013-1095-5

Coyne, J. A., & Orr, H. A. (2004). *Speciation*. Sunderland, MA: Sinauer Associates.

Da Silva, A., van den Brink, V., Emaresi, G., Luzio, E., Bize, P., Dreiss, A. N., & Roulin, A. (2013). Melanin-based

colour polymorphism signals aggressive personality in nest and territory defence in the tawny owl (Strix aluco). *Behavioral Ecology and Sociobiology*, *67*(7), 1041–1052. https://doi.org/10.1007/s00265-013-1529-2

Dasmahapatra, K. K., Blum, M. J., Aiello, A., Hackwell, S., Davies, N., Bermingham, E. P., & Mallet, J. (2002). IInferences from a rapidly moving hybrid zone. *Evolution*, *56*(4), 741–753. https://doi.org/10.1111/j.0014-3820.2002.tb01385.x

Day, L. B., Helmhout, W., Pano, G., Olsson, U., Hoeksema, J. D., & Lindsay, W. R. (2021). Correlated Evolution of Acrobatic Display and Both Neural and Somatic Phenotypic Traits in Manakins (Pipridae). *Integrative and Comparative Biology*, *61*(4), 1343–1362. https://doi.org/10.1093/icb/icab139

de Zwaan, D. R., Barnes, S., & Martin, K. (2019). Plumage melanism is linked to male quality, female parental investment and assortative mating in an alpine songbird. *Animal Behaviour*, *156*, 41–49. https://doi.org/10.1016/j.anbehav.2019.06.034

Derryberry, E. P., Derryberry, G. E., Maley, J. M., & Brumfield, R. T. (2014). hzar: hybrid zone analysis using an R software package. *Molecular Ecology Resources*, *14*(3), 652–663. https://doi.org/10.1111/1755-0998.12209

Ducrest, A., Keller, L., & Roulin, A. (2008). Pleiotropy in the melanocortin system, coloration and behavioural syndromes. *Trends in Ecology & Evolution*, *23*(9), 502–510. https://doi.org/10.1016/j.tree.2008.06.001

Engebretsen, K. N., Barrow, L. N., Rittmeyer, E. N., Brown, J. M., & Lemmon, E. M. (2016). Quantifying the spatiotemporal dynamics in a chorus frog (Pseudacris) hybrid zone over 30 years. *Ecology and Evolution*, *6*(14), 5013–5031. https://doi.org/10.1002/ece3.2232

Etter, P. D., Preston, J. L., Bassham, S., Cresko, W. A., & Johnson, E. A. (2011). Local De Novo Assembly of RAD Paired-End Contigs Using Short Sequencing Reads. *PLoS ONE*, *6*(4), e18561. https://doi.org/10.1371/journal.pone.0018561

Fordham, G., Shanee, S., & Peck, M. (2020). Effect of river size on Amazonian primate community structure: A biogeographic analysis using updated taxonomic assessments. *American Journal of Primatology*, *82*(7), e23136. https://doi.org/10.1002/ajp.23136

Fouquet, A., Ledoux, J.-B., Dubut, V., Noonan, B. P., & Scotti, I. (2012). The interplay of dispersal limitation, rivers, and historical events shapes the genetic structure of an Amazonian frog. *Biological Journal of the Linnean Society*, *106*(2), 356–373. https://doi.org/10.1111/j.1095-8312.2012.01871.x

Fridolfsson, A.-K., & Ellegren, H. (1999). A Simple and Universal Method for Molecular Sexing of Non-Ratite Birds. *Journal of Avian Biology*, *30*(1), 116. https://doi.org/10.2307/3677252

Griffith, S. C., & Hooper, D. M. (2017). Geographical variation in bill colour in the Long-tailed Finch: evidence for a narrow zone of admixture between sub-species. *Emu - Austral Ornithology*, *117*(2), 141–150. https://doi.org/10.1080/01584197.2016.1277763

Gross, B. L., & Rieseberg, L. H. (2005). The Ecological Genetics of Homoploid Hybrid Speciation. *Journal of Heredity*, *96*(3), 241–252. https://doi.org/10.1093/jhered/esi026

Haffer, J. (1997). Contact Zones between Birds of Southern Amazonia. *Ornithological Monographs*, (48), 281–305. https://doi.org/10.2307/40157539

Harr, B., & Price, T. (2014). Climate Change: A Hybrid Zone Moves North. *Current Biology*, *24*(6), R230–R232. https://doi.org/10.1016/j.cub.2014.02.023

Hohenlohe, P. A., Bassham, S., Currey, M., & Cresko, W. A. (2012). Extensive linkage disequilibrium and parallel adaptive divergence across threespine stickleback genomes. *Philosophical Transactions of the Royal Society B: Biological Sciences*, *367*(1587), 395–408. https://doi.org/10.1098/rstb.2011.0245

Jombart, T. (2008). adegenet : a R package for the multivariate analysis of genetic markers. *Bioinformatics*, *24*(11), 1403–1405. https://doi.org/10.1093/bioinformatics/btn129

Jombart, T., & Ahmed, I. (2011). adegenet 1.3-1 : new tools for the analysis of genome-wide SNP data. *Bioinformatics*, *27*(21), 3070–3071. https://doi.org/10.1093/bioinformatics/btr521

Kearns, A. M., Restani, M., Szabo, I., Schrøder-Nielsen, A., Kim, J. A., Richardson, H. M., … Omland, K. E. (2018). Genomic evidence of speciation reversal in ravens. *Nature Communications*, *9*(1), 906. https://doi.org/10.1038/s41467-018-03294-w

Kelly, R. J., Murphy, T. G., Tarvin, K. A., & Burness, G. (2012). Carotenoid-based ornaments of female and male American goldfinches (Spinus tristis) show sex-specific correlations with immune function and metabolic rate. *Physiological and Biochemical Zoology : PBZ*, *85*(4), 348–363. https://doi.org/10.1086/666059

Kirwan, G. M., & Green, G. (2011). *Cotingas and manakins*. Princeton, N.J: Princeton University Press.

Li, H., & Durbin, R. (2009). Fast and accurate short read alignment with Burrows-Wheeler transform. *Bioinformatics*, *25*(14), 1754–1760. https://doi.org/10.1093/bioinformatics/btp324

Li, H., Handsaker, B., Wysoker, A., Fennell, T., Ruan, J., Homer, N., … Durbin, R. (2009). The Sequence

Alignment/Map format and SAMtools. *Bioinformatics*, *25*(16), 2078–2079. https://doi.org/10.1093/bioinformatics/btp352

Li, Heng. (2013). Aligning sequence reads, clone sequences and assembly contigs with BWA-MEM. *ArXiv*. https://doi.org/https://doi.org/10.48550/arXiv.1303.3997

Lipshutz, S. E., Meier, J. I., Derryberry, G. E., Miller, M. J., Seehausen, O., & Derryberry, E. P. (2019). Differential introgression of a female competitive trait in a hybrid zone between sex-role reversed species. *Evolution*, *73*(2), 188–201. https://doi.org/10.1111/evo.13675

Longmire, J. L., Maltbie, M., & Baker, R. J. (1997). *Use of '"lysis buffer"' in isolation and its implications for museum collections*. *Occasional papers of the Museum of Texas Tech University* (Vol. 163). Museum of Texas Tech University.

Macholán, M., Baird, S. J., Munclinger, P., Dufková, P., Bímová, B., & Piálek, J. (2008). Genetic conflict outweighs heterogametic incompatibility in the mouse hybrid zone? *BMC Evolutionary Biology*, *8*(1), 271. https://doi.org/10.1186/1471-2148-8-271

Macholán, M., Munclinger, P., Šugerková, M., Dufková, P., Bímová, B., Božíková, E., … Piálek, J. (2007). Genetic analysis of autosomal and x-linked markers across a mouse hybrid zone. *Evolution*, *61*(4), 746–771. https://doi.org/10.1111/j.1558-5646.2007.00065.x

Mafli, A., Wakamatsu, K., & Roulin, A. (2011). Melanin-based coloration predicts aggressiveness and boldness in captive eastern Hermann's tortoises. *Animal Behaviour*, *81*(4), 859–863. https://doi.org/10.1016/j.anbehav.2011.01.025

Mateos-Gonzalez, F., & Senar, J. C. (2012). Melanin-based trait predicts individual exploratory behaviour in siskins, Carduelis spinus. *Animal Behaviour*, *83*(1), 229–232. https://doi.org/10.1016/j.anbehav.2011.10.030

McDonald, D. B., Clay, R. P., Brumfield, R. T., & Braun, M. J. (2001). Sexual selection on plumage and behavior in an avian hybrid zone: experimental tests of male-male interactions. *Evolution*, *55*(7), 1443–1451. https://doi.org/10.1111/j.0014-3820.2001.tb00664.x

McEntee, J. P., Burleigh, J. G., & Singhal, S. (2020). Dispersal Predicts Hybrid Zone Widths across Animal Diversity: Implications for Species Borders under Incomplete Reproductive Isolation. *The American Naturalist*, *196*(1), 9–28. https://doi.org/10.1086/709109

Metzler, D., Knief, U., Peñalba, J. V., & Wolf, J. B. W. (2021). Assortative mating and epistatic mating-trait architecture induce complex movement of the crow hybrid zone. *Evolution*, *75*(12), 3154–3174. https://doi.org/10.1111/evo.14386

Moore, R. P., Robinson, W. D., Lovette, I. J., & Robinson, T. R. (2008). Experimental evidence for extreme dispersal limitation in tropical forest birds. *Ecology Letters*, *11*(9), 960–968. https://doi.org/10.1111/j.1461-0248.2008.01196.x

Morales-Rozo, A., Tenorio, E. A., Carling, M. D., & Cadena, C. D. (2017). Origin and cross-century dynamics of an avian hybrid zone. *BMC Evolutionary Biology*, *17*(1), 257. https://doi.org/10.1186/s12862-017-1096-7

Moran, B. M., Payne, C., Langdon, Q., Powell, D. L., Brandvain, Y., & Schumer, M. (2021). The genomic consequences of hybridization. *ELife*, *10*. https://doi.org/10.7554/eLife.69016

Naka, L. N., Bechtoldt, C. L., Henriques, L. M. P., & Brumfield, R. T. (2012). The Role of Physical Barriers in the Location of Avian Suture Zones in the Guiana Shield, Northern Amazonia. *The American Naturalist*, *179*(4), E115–E132. https://doi.org/10.1086/664627

Naka, L. N., Costa, B. M. da S., Lima, G. R., & Claramunt, S. (2022). Riverine Barriers as Obstacles to Dispersal in Amazonian Birds. *Frontiers in Ecology and Evolution*, *10*, 539. https://doi.org/10.3389/fevo.2022.846975

Nazareno, A. G., Knowles, L. L., Dick, C. W., & Lohmann, L. G. (2021). By Animal, Water, or Wind: Can Dispersal Mode Predict Genetic Connectivity in Riverine Plant Species? *Frontiers in Plant Science*, *12*, 31. https://doi.org/10.3389/fpls.2021.626405

Ottenburghs, J., Kraus, R. H. S., van Hooft, P., van Wieren, S. E., Ydenberg, R. C., & Prins, H. H. T. (2017). Avian introgression in the genomic era. *Avian Research*, *8*(1), 30. https://doi.org/10.1186/s40657-017-0088-z

Parchman, T. L., Gompert, Z., Braun, M. J., Brumfield, R. T., McDonald, D. B., Uy, J. A. C., … Buerkle, C. A. (2013). The genomic consequences of adaptive divergence and reproductive isolation between species of manakins. *Molecular Ecology*, *22*(12), 3304–3317. https://doi.org/10.1111/mec.12201

Parsons, T. J., Olson, S. L., & Braun, M. J. (1993). Unidirectional Spread of Secondary Sexual Plumage Traits Across an Avian Hybrid Zone. *Science*, *260*(5114), 1643–1646. https://doi.org/10.1126/science.260.5114.1643

Payseur, B. A., & Rieseberg, L. H. (2016). A genomic perspective on hybridization and speciation. *Molecular Ecology*, *25*(11), 2337–2360. https://doi.org/10.1111/MEC.13557

Phillips, B. L., Baird, S. J. E., & Moritz, C. (2004). When vicars meet: a narrow contact zone between

morphologically cryptic phylogeographic lineages of the rainforest skink, Carlia rubrigularis. *Evolution*, *58*(7), 1536–1548. https://doi.org/10.1111/j.0014-3820.2004.tb01734.x

Pinto, B. J., Titus-McQuillan, J., Daza, J. D., & Gamble, T. (2019). Persistence of a Geographically-Stable Hybrid Zone in Puerto Rican Dwarf Geckos. *Journal of Heredity*, *110*(5), 523–534. https://doi.org/10.1093/jhered/esz015

R Core Team. (2022). R: A language and environment for statistical computing. Vienna, Austria: R Foundation for Statistical Computing. Retrieved from https://www.r-project.org/

Reudink, M. W., Mech, S. G., Mullen, S. P., & Curry, R. L. (2007). Structure and Dynamics of The Hybrid Zone Between Black-Capped Chickadee (Poecile Atricapillus) and Carolina Chickadee (P. Carolinensis) in Southeastern Pennsylvania. *The Auk*, *124*(2), 463–478. https://doi.org/10.1093/auk/124.2.463

Roberts, N. S., & Mendelson, T. C. (2020). Reinforcement in the banded darter Etheostoma zonale : The effect of sex and sympatry on preferences. *Ecology and Evolution*, *10*(5), 2499–2512. https://doi.org/10.1002/ece3.6076

Rochette, N. C., Rivera-Colón, A. G., & Catchen, J. M. (2019). Stacks 2: Analytical methods for paired-end sequencing improve RADseq-based population genomics. *Molecular Ecology*, *28*(21), 4737–4754. https://doi.org/10.1111/mec.15253

Rosser, N., Dasmahapatra, K. K., & Mallet, J. (2014). Stable Heliconius butterfly hybrid zones are correlated with a local rainfall peak at the edge of the Amazon basin. *Evolution*, *68*(12), 3470–3484. https://doi.org/10.1111/evo.12539

Rosser, N., Shirai, L. T., Dasmahapatra, K. K., Mallet, J., & Freitas, A. V. L. (2021). The Amazon river is a suture zone for a polyphyletic group of co-mimetic heliconiine butterflies. *Ecography*, *44*(2), 177–187. https://doi.org/10.1111/ECOG.05282

Ruegg, K. (2008). Genetic, morphological, and ecological characterization of a hybrid zone that spans a migratory divide. *Evolution*, *62*(2), 452–466. https://doi.org/10.1111/j.1558-5646.2007.00263.x

Seehausen, O., Alphen, J. J. M. van, & Witte, F. (1997). Cichlid Fish Diversity Threatened by Eutrophication That Curbs Sexual Selection. *Science*, *277*(5333), 1808–1811. https://doi.org/10.1126/science.277.5333.1808

Semenov, G. A., Linck, E., Enbody, E. D., Harris, R. B., Khaydarov, D. R., Alström, P., … Taylor, S. A. (2021). Asymmetric introgression reveals the genetic architecture of a plumage trait. *Nature Communications*, *12*(1). https://doi.org/10.1038/S41467-021-21340-Y

Smith, K. L., Hale, J. M., Kearney, M. R., Austin, J. J., & Melville, J. (2013). Molecular patterns of introgression in a classic hybrid zone between the Australian tree frogs, Litoria ewingii and L. paraewingi : evidence of a tension zone. *Molecular Ecology*, *22*(7), 1869–1883. https://doi.org/10.1111/mec.12176

Snow, D. (2004). Family Pipridae (Manakins). In J. del Hoyo, A. Elliott, & D. A. Christie (Eds.), *Handbook of the birds of the world. Vol. 9. Cotingas to pipits and wagtails* (pp. 110–169). Barcelona: Lynx Edicions.

Stein, A. C., & Uy, J. A. C. (2006a). Plumage brightness predicts male mating success in the lekking golden-collared manakin, Manacus vitellinus. *Behavioral Ecology*, *17*(1), 41–47. https://doi.org/10.1093/beheco/ari095

Stein, A. C., & Uy, J. A. C. (2006b). Unidirectional introgression of a sexually selected trait across an avian hybrid zone: A role for female choice? *Evolution*, *60*(7), 1476–1485. https://doi.org/10.1111/j.0014-3820.2006.tb01226.x

Szymura, J. M., & Barton, N. H. (1986). Genetic Analysis of a Hybrid Zone Between the Fire-Bellied Toads, Bombina Bombina and B. Variegata, Near Cracow in Southern Poland. *Evolution*, *40*(6), 1141–1159. https://doi.org/10.1111/j.1558-5646.1986.tb05740.x

Szymura, J. M., & Barton, N. H. (1991). The genetic structure of the hybrid zone between the fire-bellied toads Bombina bombina and B. Variegata: Comparisons between transects and between loci. *Evolution*, *45*(2), 237–261. https://doi.org/10.1111/j.1558-5646.1991.tb04400.x

Taylor, S. A., & Larson, E. L. (2019). Insights from genomes into the evolutionary importance and prevalence of hybridization in nature. *Nature Ecology & Evolution*, *3*(2), 170–177. https://doi.org/10.1038/s41559-018-0777-y

Taylor, S. A., White, T. A., Hochachka, W. M., Ferretti, V., Curry, R. L., & Lovette, I. (2014). Climate-Mediated Movement of an Avian Hybrid Zone. *Current Biology*, *24*(6), 671–676. https://doi.org/10.1016/j.cub.2014.01.069

Trigo, T. C., Schneider, A., de Oliveira, T. G., Lehugeur, L. M., Silveira, L., Freitas, T. R. O., & Eizirik, E. (2013). Molecular Data Reveal Complex Hybridization and a Cryptic Species of Neotropical Wild Cat. *Current Biology*, *23*(24), 2528–2533. https://doi.org/10.1016/j.cub.2013.10.046

Walsh, J., Billerman, S. M., Rohwer, V. G., Butcher, B. G., & Lovette, I. J. (2020). Genomic and plumage variation across the controversial Baltimore and Bullock's oriole hybrid zone. *The Auk*, *137*(4), 1–15.

https://doi.org/10.1093/AUK/UKAA044

Wang, N., Borrell, J. S., Bodles, W. J. A., Kuttapitiya, A., Nichols, R. A., & Buggs, R. J. A. (2014). Molecular footprints of the Holocene retreat of dwarf birch in Britain. *Molecular Ecology*, *23*(11), 2771–2782. https://doi.org/10.1111/mec.12768

Wang, S., Rohwer, S., Delmore, K., & Irwin, D. E. (2019). Cross-decades stability of an avian hybrid zone. *Journal of Evolutionary Biology*, *32*(11), 1242–1251. https://doi.org/10.1111/jeb.13524

Wielstra, B. (2019). Historical hybrid zone movement: More pervasive than appreciated. *Journal of Biogeography*, *46*(7), 1300–1305. https://doi.org/10.1111/jbi.13600

Wielstra, B., Burke, T., Butlin, R. K., & Arntzen, J. W. (2017). A signature of dynamic biogeography: enclaves indicate past species replacement. *Proceedings of the Royal Society B: Biological Sciences*, *284*(1868), 20172014. https://doi.org/10.1098/rspb.2017.2014

Yang, W., Feiner, N., Salvi, D., Laakkonen, H., Jablonski, D., Pinho, C., … Uller, T. (2022). Population Genomics of Wall Lizards Reflects the Dynamic History of the Mediterranean Basin. *Molecular Biology and Evolution*, *39*(1), 2021. https://doi.org/10.1093/MOLBEV/MSAB311

Yang, W., While, G. M., Laakkonen, H., Sacchi, R., Zuffi, M. A. L., Scali, S., … Uller, T. (2018). Genomic evidence for asymmetric introgression by sexual selection in the common wall lizard. *Molecular Ecology*, *27*(21), 4213–4224. https://doi.org/10.1111/MEC.14861

Yuri, T., Jernigan, R. W., Brumfield, R. T., Bhagabati, N. K., & Braun, M. J. (2009). The effect of marker choice on estimated levels of introgression across an avian (Pipridae: Manacus) hybrid zone. *Molecular Ecology*, *18*(23), 4888–4903. https://doi.org/10.1111/j.1365-294X.2009.04381.x

Zohren, J., Wang, N., Kardailsky, I., Borrell, J. S., Joecker, A., Nichols, R. A., & Buggs, R. J. A. (2016). Unidirectional diploid-tetraploid introgression among British birch trees with shifting ranges shown by restriction site-associated markers. *Molecular Ecology*, *25*(11), 2413–2426. https://doi.org/10.1111/mec.13644

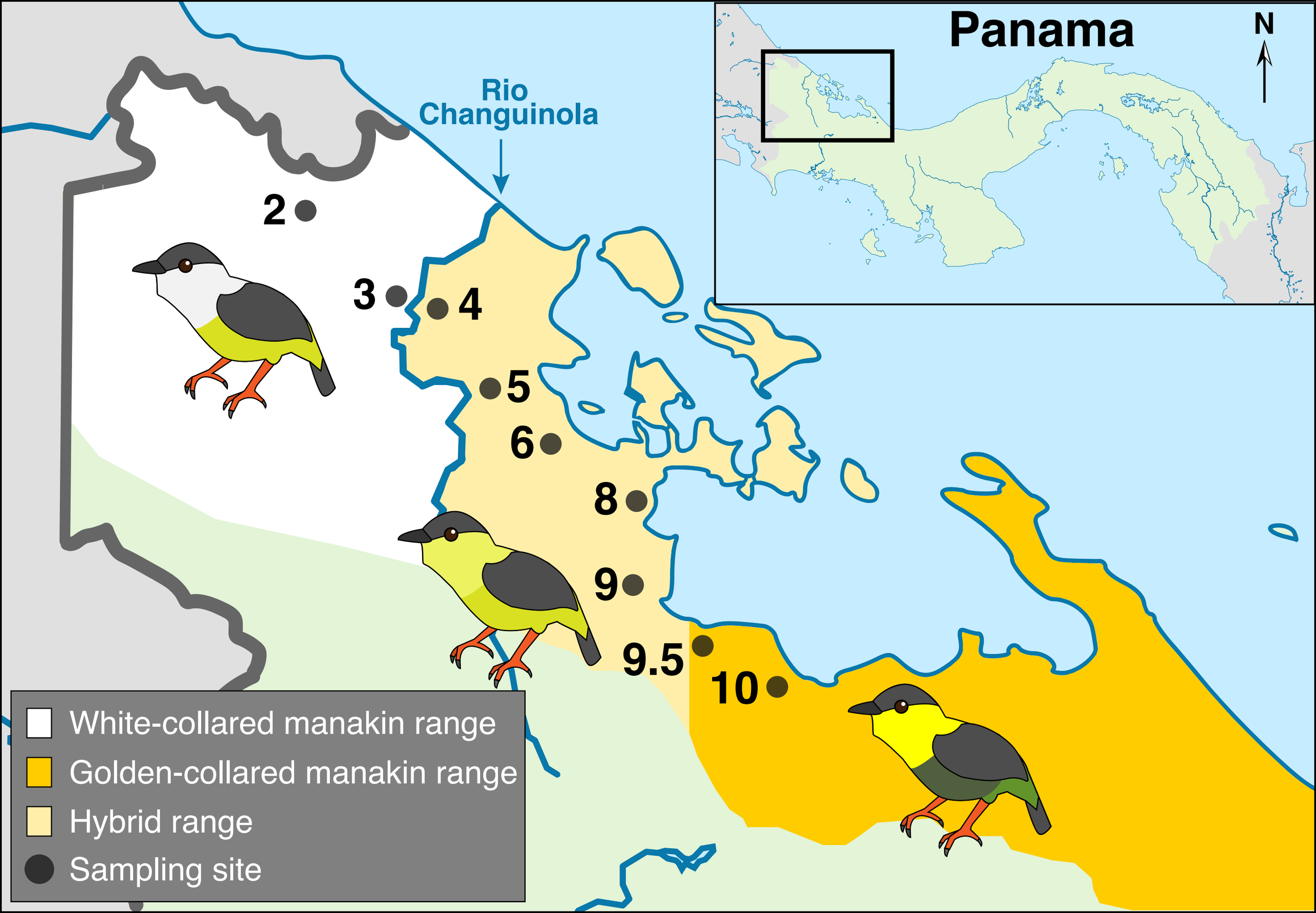
Panama
N
Rio
Changuinola
2
3
4
5
6
8
9
9.5
10
White-collared manakin range
Golden-collared manakin range
Hybrid range
Sampling site

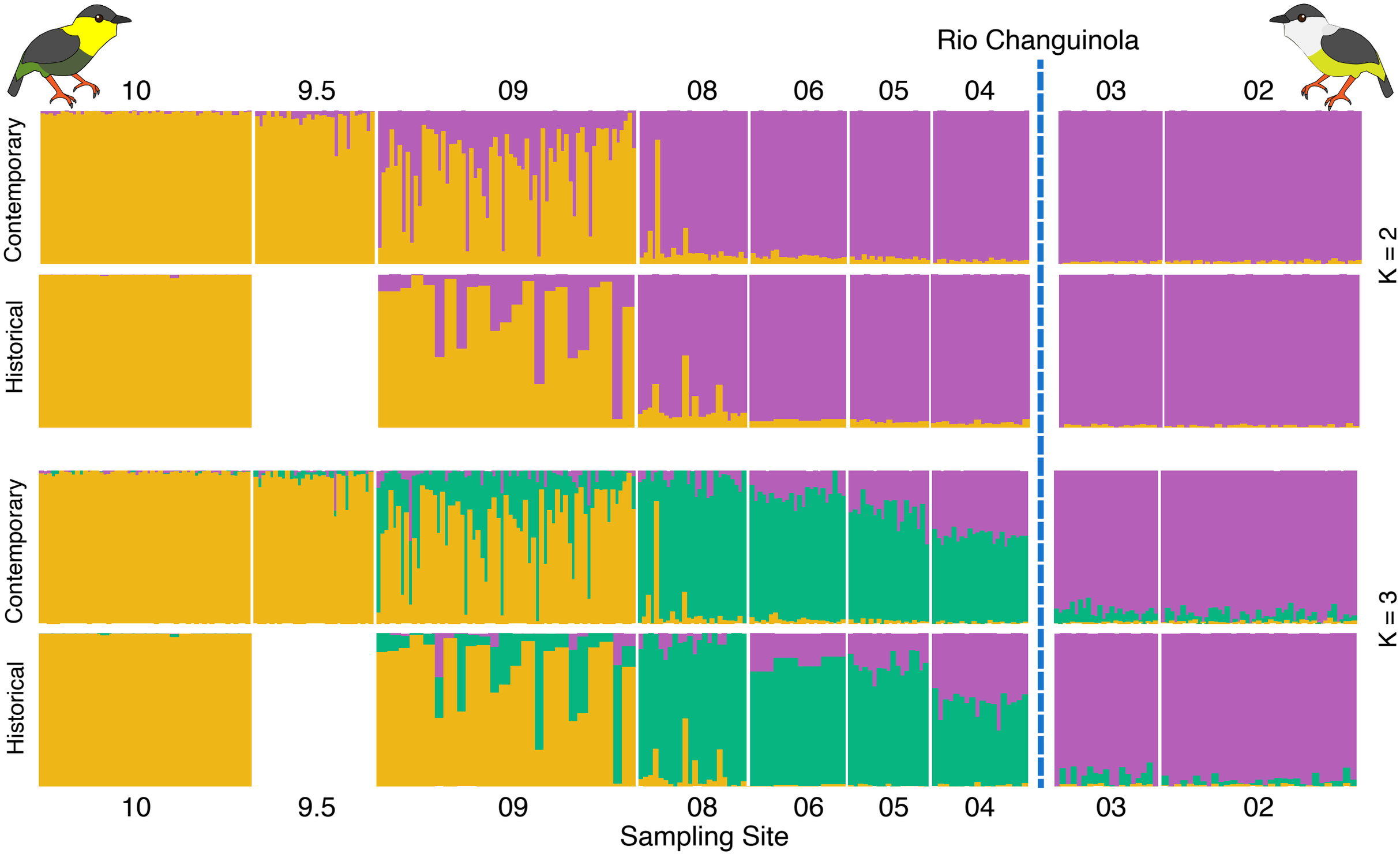
Rio Changuinola
10
9.5
09
08
06
05
04
03
02
Contemporary
Historical
K = 2
Contemporary
Historical
K = 3
10
9.5
09
08
06
05
04
03
02
Sampling Site

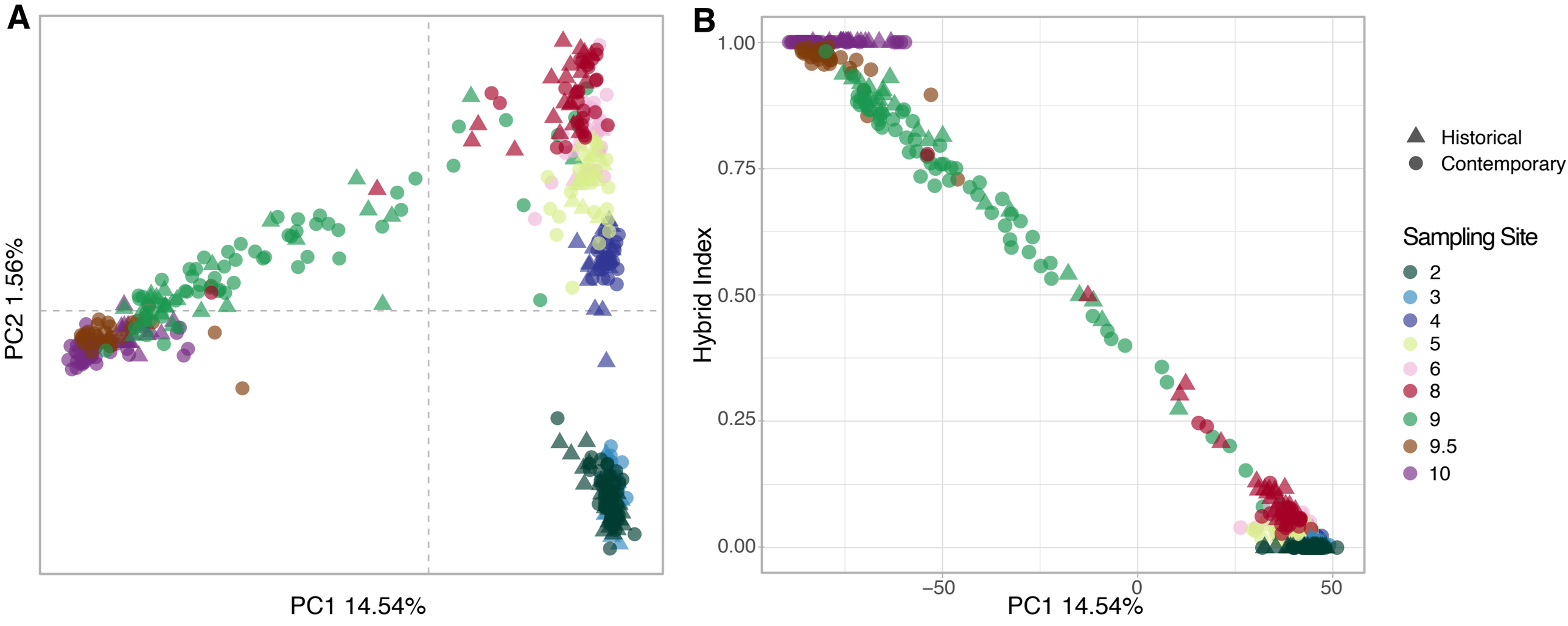
A
PC2 1.56%
PC1 14.54%
B
Hybrid Index
1.00
0.75
0.50
0.25
0.00
−50
0
50
PC1 14.54%
Historical
Contemporary
Sampling Site
2
3
4
5
6
8
9
9.5
10

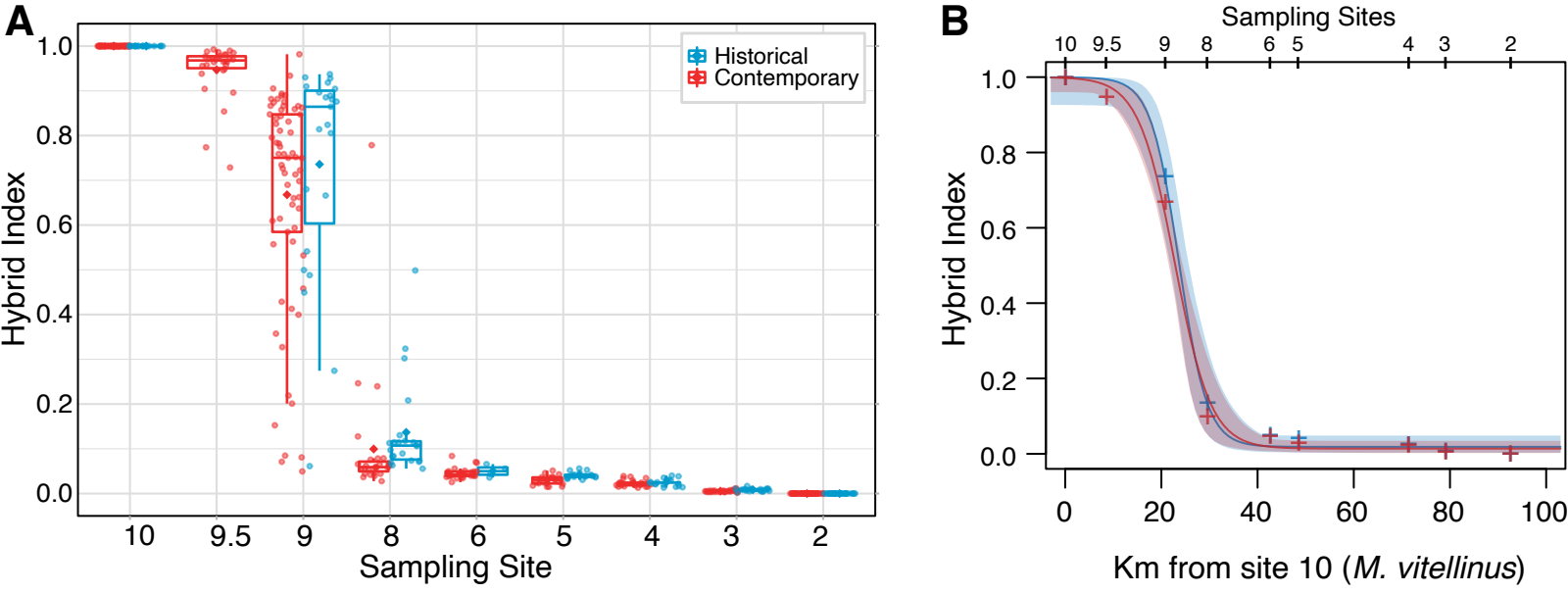
A
Hybrid Index
1.0
0.8
0.6
0.4
0.2
0.0
Historical
Contemporary
10
9.5
9
8
6
5
4
3
2
Sampling Site
B
Sampling Sites
10
9.5
9
8
6
5
4
3
2
Hybrid Index
1.0
0.8
0.6
0.4
0.2
0.0
0
20
40
60
80
100
Km from site 10 (*M. vitellinus*)

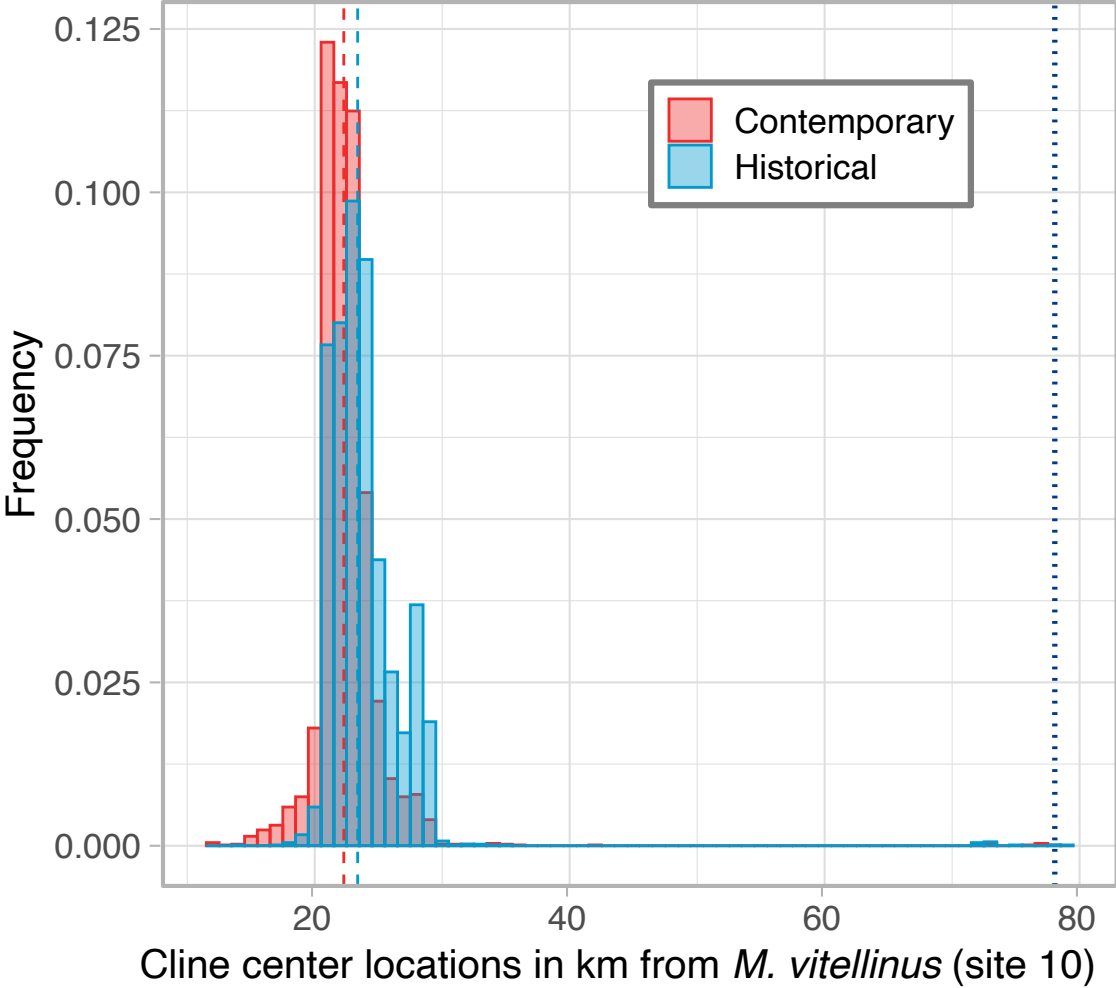
Contemporary
Historical
Frequency
0.125
0.100
0.075
0.050
0.025
0.000
20
40
60
80
Cline center locations in km from *M. vitellinus* (site 10)

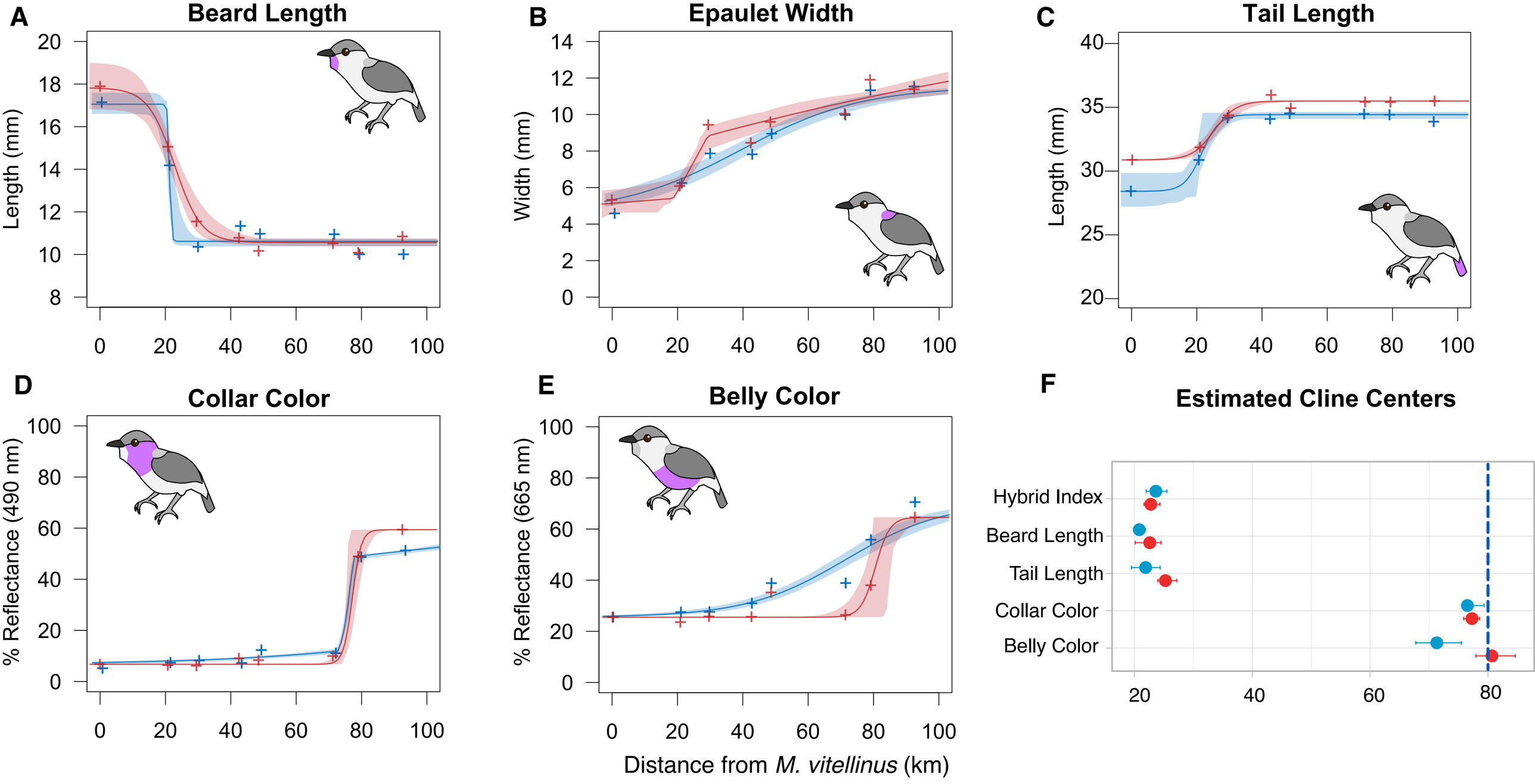
A
Beard Length
Length (mm)
B
Epaulet Width
Width (mm)
C
Tail Length
Length (mm)
D
Collar Color
% Reflectance (490 nm)
E
Belly Color
% Reflectance (665 nm)
Distance from M. vitellinus (km)
F
Estimated Cline Centers
Hybrid Index
Beard Length
Tail Length
Collar Color
Belly Color